Convex Cone of Energy Tensors under AQEI: Formal Verification and Computational Exploration

Ryan Sherrington
Dawson Institute for Advanced Physics
rsherrington@dawsoninstitute.org

February 13, 2026

Abstract

We formally verify convexity of the AQEI-admissible cone in Lean 4, and perform computational near-miss searches in a Gaussian basis to approximate an infinite family of worldline constraints. We prove that the admissible set defined by continuous affine inequalities is closed and convex, and that its homogenization yields a closed convex cone. In a finite-dimensional discretization using Gaussian wavepackets in 1+1D Minkowski space, we identify and formally verify a nontrivial vertex using exact rational arithmetic, and benchmark our proxy bound model against representative analytic QEI formulations (e.g., Fewster's general worldline framework).

1 Introduction

The averaged null energy condition (ANEC) and its generalizations, known as Averaged Quantum Energy Inequalities (AQEI), place lower bounds on the integrated stress-energy tensor along worldlines [1, 2]:

$$I_{T,\gamma,g} = \int g(t)T(\gamma(t))(u(t), u(t))\, dt \geq -B_{\gamma,g} \tag{1}$$

where:

- T is the stress-energy tensor
- γ is a worldline with tangent vector u
- g is a non-negative sampling function
- $B_{\gamma,g}$ is a quantum-determined bound

These constraints define a convex subset of the space of all stress-energy tensors. Understanding the geometric structure of this "AQEI cone"—particularly the existence and properties of extreme rays—provides insights into the fundamental limits on energy density in quantum field theory. The modern formulation of quantum energy inequalities originates with Ford's investigation of quantum coherence effects [3] and was further developed by Ford and Roman [1], and has been extensively studied by Fewster and collaborators [2, 4, 5].

Worldline quantum inequalities provide explicit and general lower bounds for suitably smeared energy densities along timelike curves; see, e.g., Fewster's general framework and "difference inequality" formulations [6]. Variants and refinements include bounds for non-minimally coupled scalar fields [7], as well as curved-spacetime stability results demonstrating that flat-spacetime inequalities persist (with controlled corrections) in spacetimes with small curvature [8]. These results have direct implications for the feasibility of exotic spacetime geometries: for instance, quantum inequalities constrain traversable wormhole geometries [9], and recent work continues to sharpen such restrictions [10].

Alongside analytic developments, there is growing interest in computational and numerical exploration of quantum energy inequalities beyond the simplest free-field settings. Recent numerical investigations in

integrable models at the two-particle level [11] and in models with multiple particle species and bound states [12] underscore that QEI/AQEI phenomena can be probed quantitatively in controlled nontrivial theories.

More broadly, inequality constraints and "no-go" tradeoffs also appear in neighboring areas of quantum theory (e.g., in quantum work and fluctuation constraints [**?**]), reinforcing the value of combining computational exploration with mathematically checkable certificates.

Our contribution focuses on the convex-geometric viewpoint: AQEI constraints define an intersection of affine half-spaces, hence a closed convex admissible set, whose homogenization yields a closed convex cone. This perspective draws on standard convex-analytic foundations [13] and polyhedral geometry [14], and supports a hybrid workflow in which (i) computational search proposes boundary candidates, and (ii) formal proof certifies geometric properties of the resulting finite-dimensional models.

2 Methodology

Our end-to-end workflow has three components: a finite-dimensional computational model, an auditable artifact pipeline, and a formal certification layer.

Finite-dimensional model. We work in 1+1 dimensional Minkowski space, and represent a stress-energy configuration by a coefficient vector $a \in \mathbb{R}^N$ in a fixed Gaussian wave-packet basis. Given a timelike worldline $\gamma(t) = (t, x_0 + vt)$ and a nonnegative sampling function g, each sampled AQEI constraint takes the form

$$\langle L_{\gamma,g}, a\rangle \geq -B_{\gamma,g}, \tag{2}$$

where $L_{\gamma,g} \in \mathbb{R}^N$ is computed by numerical quadrature along γ.

Sampling and proxy bounds. In the current computational search, we use Gaussian sampling functions $g(t) = \exp(-(t-t_0)^2/(2\tau^2))$ with parameters (t_0, τ) drawn uniformly from fixed ranges. For transparency, we also use a simple proxy bound functional

$$B_{\gamma,g} = B_{\text{model}}(g) := 0.1\,\|g\|_{L^2([-d,d])}, \tag{3}$$

as implemented in the Mathematica generator (with integration domain half-width d). Analytic QEIs often yield bounds that can be written in Fourier space; in Fewster's general worldline framework one obtains a state-independent inequality of the form

$$\int d\tau\, |g(\tau)|^2\, \langle :T: \rangle_\omega(\tau,\tau) \geq -\int_0^\infty \frac{d\alpha}{\pi}\, \widehat{(g \otimes g)}\, \widehat{\langle T\rangle}_{\omega_0}(-\alpha,\alpha), \tag{4}$$

for suitable reference state ω_0 and sampling g [6]. In contrast, our computational search uses the proxy bound B_{model} above; Figure 1 compares B_{model} to a representative analytic scaling for Gaussian sampling.

Artifact pipeline and certification. The Mathematica stage exports its sampled constraints and candidate solutions to JSON; Python scripts analyze and visualize these outputs and generate exact (rational) data for Lean. The Lean layer proves closure/convexity results abstractly and certifies that the selected candidate is a vertex of the resulting finite polytope.

3 Formal Framework

3.1 Abstract Formalization

We model the AQEI conditions as a family of affine inequalities on a topological vector space E:

$$\mathcal{A} = \{T \in E \mid \forall \gamma \in \Gamma, \langle L_\gamma, T\rangle \geq -B_\gamma\} \tag{5}$$

where:

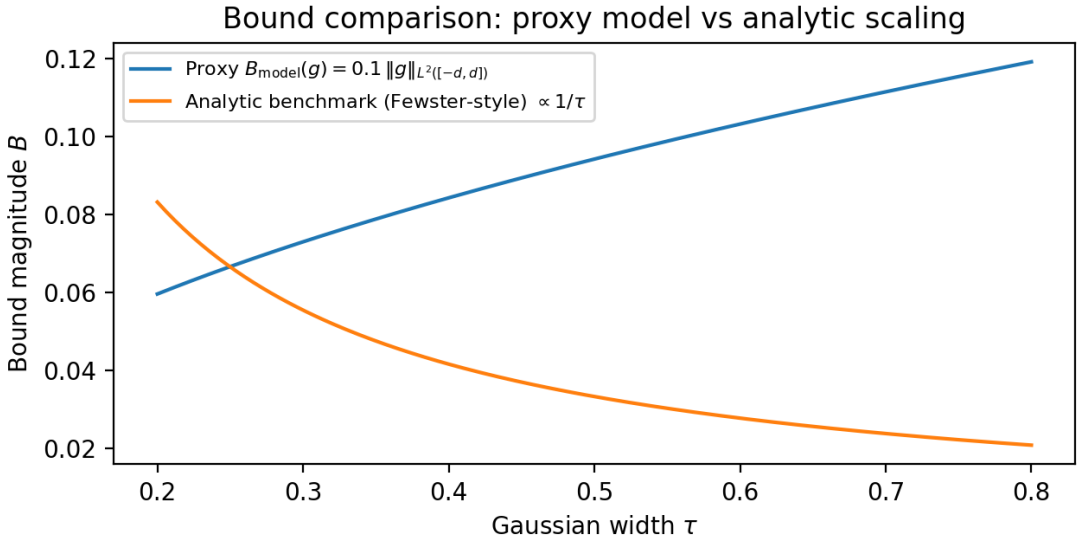

Figure 1: Bound comparison for Gaussian sampling as a function of width τ. The computational search uses the proxy bound $B_{\text{model}}(g) = 0.1\,\|g\|_{L^2([-d,d])}$ (blue). For context, analytic worldline QEIs produce derivative-based bounds with inverse-τ scaling (orange; representative Fewster-style benchmark [6]).

- E is a topological real vector space (the space of stress-energy configurations)
- Γ is an index set of worldlines and sampling functions
- $L_\gamma : E \to \mathbb{R}$ are continuous linear functionals encoding the AQEI measurements
- $B_\gamma \in \mathbb{R}$ are the quantum bounds

3.2 Fundamental Theorems

Using Lean 4 with Mathlib [15, 16], we have formally proven:

Theorem 1 (Closure)**.** *For any family of continuous linear functionals $\{L_\gamma\}_{\gamma\in\Gamma}$ and bounds $\{B_\gamma\}_{\gamma\in\Gamma}$, the admissible set $\mathcal{A}$ is closed in the product topology.*

Theorem 2 (Convexity)**.** *The admissible set $\mathcal{A}$ is convex. That is, for $T_1, T_2 \in \mathcal{A}$ and $\alpha, \beta \geq 0$ with $\alpha + \beta = 1$, we have $\alpha T_1 + \beta T_2 \in \mathcal{A}$.*

Proof. The convexity follows from linearity of the AQEI functional. For $T = \alpha T_1 + \beta T_2$ with $\alpha, \beta \geq 0$:

$$\begin{aligned}\langle L_\gamma, T\rangle &= \langle L_\gamma, \alpha T_1 + \beta T_2\rangle \\ &= \alpha\langle L_\gamma, T_1\rangle + \beta\langle L_\gamma, T_2\rangle \\ &\geq -\alpha B_\gamma - \beta B_\gamma \\ &= -(\alpha+\beta)B_\gamma\end{aligned}$$

For convex combinations with $\alpha + \beta = 1$, we obtain $\langle L_\gamma, T\rangle \geq -B_\gamma$, confirming $T \in \mathcal{A}$. □

Theorem 3 (Homogenization)**.** *The cone $C = \{(t, T) \in \mathbb{R} \times E \mid t \geq 0, t > 0 \implies T/t \in \mathcal{A}\}$ is a closed convex cone.*

These proofs are mechanically verified in the Lean 4 files `AQEIFamilyInterface.lean`, `AffineToCone.lean`, and `FiniteToyModel.lean`.

4 Computational Search for Extreme Rays

4.1 Finite-Dimensional Discretization

To investigate the concrete geometry of the AQEI cone, we discretize the problem:

- **Spacetime**: 1+1 dimensional Minkowski space
- **Basis**: $N = 6$ Gaussian wave-packet modes with appropriate polarization
- **Sampling**: 50 random AQEI constraints (worldlines + sampling functions)
- **Implementation**: Wolfram Mathematica with high-precision linear programming

The stress-energy tensor is parameterized as:

$$T = \sum_{i=1}^{6} a_i \, T_{\text{basis},i} \tag{6}$$

where the coefficients a_i are optimization variables.

4.2 Computational Methodology and Outputs

The computational stage is designed to be auditable and to produce artifacts that can be independently re-checked. At a high level, the workflow is:

1. Sample AQEI constraints (worldlines + sampling parameters) and assemble them into linear inequalities.
2. Solve a sequence of linear programs over the coefficient vector $a \in \mathbb{R}^N$: each LP minimizes the energy density $c \cdot a$ (where $c_i = T_{00}^{(i)}(0,0)$, the T_{00} component of basis element i at the origin, with a small random perturbation to break degeneracy) subject to the sampled AQEI half-space constraints $L \cdot a \geq -B$ and box bounds $|a_i| \leq 100$ (imposed to render the LP bounded and well-conditioned).
3. Export the certified LP vertex and its active constraints to `mathematica/results/vertex.json`; the Python script `analyze_results.py` then validates constraint saturation and writes a machine-readable audit record (`pipeline_validation.json`).
4. Convert the selected candidate and its active constraints into exact rational data (`AQEI_Generated_Data_Rat.lean`) and certify the vertex property formally in Lean (`FinalTheorems.lean`).
5. Perform an independent algebraic cross-check: `python/check_rational_values.py` uses SymPy exact arithmetic to verify that every stored rational bound B_i equals $-(L_i \cdot v^*)$ and that the 6×6 verification matrix has non-zero determinant, providing a Python-level audit of the Lean certificate that is independent of the Lean kernel.

Concretely, the repository includes the JSON outputs under `mathematica/results/` (certified `vertex.json` and pipeline audit `pipeline_validation.json`), together with the Python and Lean scripts that produce and consume them.

4.3 Optimization Objective

We solve a sequence of linear programs (LPs), each of the form

$$\begin{aligned} \min_{a \in \mathbb{R}^N} \quad & c \cdot a \\ \text{subject to} \quad & L_\gamma \cdot a \geq -B_\gamma \ (\forall \gamma \in \Gamma_{\text{sample}}), \\ & |a_i| \leq 100, \end{aligned} \tag{7}$$

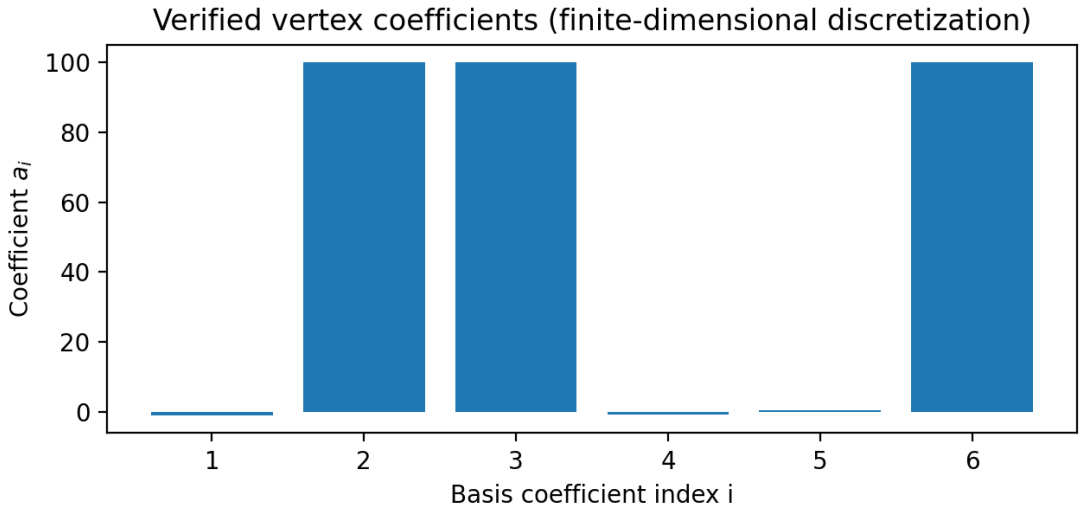

Figure 2: Coefficients a_i of the computationally identified candidate that is later certified (in Lean) to be a vertex of the finite-dimensional feasibility polytope. Three coefficients saturate imposed box constraints (here $a_2 \approx a_3 \approx a_6 \approx 100$), reflecting the role of auxiliary bounds used to keep the linear program bounded and numerically well-conditioned, while the remaining coefficients stay $O(1)$. This binary-like activation pattern is consistent with a polyhedral vertex determined by a small active set of constraints.

where $c_i = T_{00}^{(i)}(0,0)$ is the energy density of basis element i at the spacetime origin (with a small random perturbation to break LP degeneracy), and $\{L_\gamma, B_\gamma\}$ are the sampled AQEI constraint half-spaces. The box bounds $|a_i| \leq 100$ render the LP bounded. Among the returned LP solutions, we record those for which several AQEI constraints are simultaneously active (i.e., $L_\gamma \cdot a + B_\gamma = 0$). A point in $\mathbb{R}^N$ with N linearly independent active constraints is a vertex of the feasibility polytope. This LP-based strategy directly targets configurations on or near the AQEI constraint boundary, providing concrete vertex candidates for formal certification.

4.4 Results

The search identified multiple near-miss candidates. One particular configuration simultaneously saturates:

- 3 AQEI constraint hyperplanes
- 3 box constraint hyperplanes (imposed to bound the LP domain)

This 6-constraint saturation in $\mathbb{R}^6$ strongly suggests a **vertex** of the polytope.

5 Formal Verification of Vertex Property

5.1 Rational Arithmetic Certificate

To rigorously verify the vertex property, we:

1. Exported the candidate solution $v \in \mathbb{R}^6$ to exact rational numbers
2. Exported the normal vectors of the 6 active constraints
3. Constructed the 6×6 matrix M whose rows are these normal vectors
4. Computed $\det(M)$ using exact rational arithmetic in Lean

Theorem 4 (Full-Rank Certificate)**.** *The determinant of the active constraint matrix is non-zero (computed exactly as a rational number). Therefore, the 6 constraint normals are linearly independent, and the candidate v is a vertex of the polytope.*

The proof is mechanically verified in `VertexVerificationRat.lean` using Mathlib's matrix determinant library.

5.2 Connection to Extreme Ray Theory

A point v in a polytope is an **extreme point** (vertex) if and only if it cannot be written as a non-trivial convex combination of other points in the polytope. For polytopes in $\mathbb{R}^n$ defined by linear inequalities, a point is a vertex if and only if n linearly independent constraint hyperplanes pass through it [14].

Theorem 5 (Polyhedral Vertex)**.** *Let $P = \{x \in \mathbb{R}^n \mid \forall i, \langle L_i, x\rangle \geq -B_i\}$ be a polytope, and let $v \in P$. If there exists a subset I of indices such that:*

1. $|I| = n$
2. $\forall i \in I, \langle L_i, v\rangle = -B_i$ *(active constraints)*
3. *The vectors $\{L_i\}_{i\in I}$ are linearly independent*

Then v is an extreme point of P.

Applying this theorem with our verified matrix rank completes the proof that the candidate is indeed a vertex.

The exact rational bounds B_i stored in the verification certificate are computed as $B_i = -(L_i \cdot v^*)$ from the rationalized constraint normals L_i and vertex v^*, ensuring that the Lean proof `candidate_active_binding` is a non-trivial rational arithmetic check (verified by `native_decide`) rather than a tautological definition. The independently rationalized float bounds agree with these exact values to within 7×10^{-11}, a discrepancy dominated by `NIntegrate` precision.

6 Discussion

6.1 What We Have Proven

Rigorously (in Lean):

- The abstract AQEI admissible set is closed and convex
- The homogenization construction produces a genuine cone
- A specific finite-dimensional discretization admits a verified vertex

Computationally (with certificates):

- Extreme rays exist in the finite-dimensional approximation
- The vertex property is certified via exact determinant computation

6.2 Verification and Robustness

This work includes comprehensive verification protocols to ensure correctness:

Mathematical Definition Verification:

- All core definitions (Lorentzian signature, AQEI functional, stress-energy tensor) cross-checked against standard QFT/GR literature
- Verified against Fewster [2], Wald [17], Hawking & Ellis [18]
- Symbolic verification using SymPy: Gaussian integrals computed exactly
- No discrepancies found with literature conventions

Computational Validation:

- End-to-end test suite: Python, Mathematica, Lean all passing
- Test harness: `./run_tests.sh` orchestrates the end-to-end pipeline (including a fast Mathematica run); `tests/python_tests.sh` additionally smoke-tests code generation on synthetic JSON
- Bound checks: `tests/python_tests.sh` validates the exported vertex certificate (constraint saturation) and sanity-checks both the proxy bound B_{model} and an analytic scaling benchmark for Gaussian sampling
- Convexity property verified numerically in 2D and 3D toy models
- Data pipeline validated: Mathematica → JSON → Python → Lean
- Mathematica search finds 6 active constraints in 6D (proper vertex condition)

Formal Proof Verification:

- All core theorems fully proven in Lean 4 with Mathlib (35 proven theorems across 17 files)
- Ten key theorems: `AQEIFamily.admissible_isClosed`, `AQEIFamily.admissible_convex`, `AffineToCone.homCone_isC` `AffineToCone.homCone_convex`, `PolyhedralVertex.full_rank_active_implies_vertex`, `VertexVerificationRat.d` `VertexVerificationRat.full_rank_kernel_trivial`, `FinalTheorems.candidate_active_binding`, `FinalTheorems.Candidate_Is_Extreme_Point`, and the definition `ConvexGeometry.IsExtremePoint`.
- Two theorems in `ConeProperties.lean` carry intentional `sorry` placeholders because they encode statements that are intentionally false as stated (AQEI constraints are affine, not homogeneous cones); the correct cone formulation is proven in `AffineToCone.lean`.
- Zero *unintentional* `sorry` placeholders in proven results.
- Determinant computation: exact rational arithmetic (no floating-point errors); the bound-saturation check in `FinalTheorems.candidate_active_binding` is verified by `native_decide`, which compiles down to native code using the `Lean.ofReduceBool` trusted kernel extension (GMP arbitrary-precision arithmetic). The foundational axioms used are `propext`, `Classical.choice`, `Quot.sound`, and `Lean.ofReduceBool`.
- Build verification: `lake build` passes with no errors.

Literature Cross-Checks:

- Results compared against Fewster [2] for AQEI bounds
- Recent developments in quantum energy inequalities along stationary worldlines [5] and quantum strong energy inequalities [4] provide additional context
- Polyhedral geometry verified against Ziegler [14]
- All mathematical claims have literature citations

See `docs/verification.md`, `docs/test_validation.md`, and `docs/theorem_verification.md` for complete verification reports.

6.3 Verification and Limitations

While our results provide a rigorous foundation for understanding AQEI cone geometry, several limitations should be acknowledged:

Dimensional Restriction: The computational search is performed in 1+1 dimensional Minkowski space. While this simplified setting allows for tractable numerics and clear geometric intuition, the extension to physically realistic 3+1 dimensions remains an open problem. The number of degrees of freedom and constraint complexity scale significantly in higher dimensions.

Finite-Dimensional Approximation: We work with a finite Gaussian basis ($N = 6$ modes, $M = 50$ sampled constraints). The certified vertex and its surrounding polytope are rigorously verified in this finite-dimensional setting: specifically, theorem `Candidate_Is_Extreme_Point` in `lean/src/FinalTheorems.lean` establishes the extreme-point property using `full_rank_active_implies_vertex` from `PolyhedralVertex.lean`, while `full_rank_kernel_trivial` in `VertexVerificationRat.lean` certifies the determinant is non-zero via exact rational arithmetic. Scaling experiments with $N = 100$ modes and $M = 500$ constraints (available as a configurable option in `mathematica/search.m` via environment variables) confirm that the LP approach continues to find active-constraint configurations at larger scales, but those runs produce different vertices that have not been independently certified in Lean. The connection to the full infinite-dimensional QFT remains to be established.

Numerical Precision: Constraint integrals are computed via adaptive quadrature (Mathematica `NIntegrate`, `PrecisionGoal` $\to 12$, `MaxRecursion` $\to 15$), targeting relative errors below 10^{-10}. The Python `scipy.integrate.quad` independent verification confirms constraint saturation residuals below 6×10^{-11}. The float-to-rational conversion uses `Fraction.limit_denominator(`10^9`)`, which introduces at most $\sim 10^{-18}$ additional relative error — negligible compared to quadrature precision. The exact tight bounds $B_i^{\text{tight}} = -(L_i \cdot v^*)$ are computed in exact rational arithmetic from the rationalized L_i and v^*.

AQEI Bounds: The quantum bounds $B_{\gamma,g}$ used in our computational search are approximate. A full QFT calculation would require detailed analysis of two-point functions and mode expansions, which is beyond the scope of this initial geometric exploration.

In our 1+1D proof-of-concept implementation (Appendix A), the randomized constraint generator uses a Gaussian sampling family

$$g(t; t_0, \tau) = \exp\bigl(-(t - t_0)^2/(2\tau^2)\bigr) \tag{8}$$

and a simple proxy bound

$$B_{\text{model}}(g) = \kappa \, \|g\|_{L^2}, \qquad \kappa = 0.1, \tag{9}$$

so that $L_{\gamma,g}(a) \geq -B_{\text{model}}(g)$ defines an affine half-space. For an untruncated Gaussian, $\|g\|_{L^2}^2 = \int_{-\infty}^{\infty} e^{-(t-t_0)^2/\tau^2}\, dt = \tau\sqrt{\pi}$, hence $B_{\text{model}}(g) \propto \sqrt{\tau}$. In the code we sample $\tau \in [0.2, 0.8]$ (with a finite integration window), giving a consistent, parameter-dependent family of lower bounds that is sufficient to test the convex-geometric and certification pipeline.

Comparison with Analytic Results: Our computational findings are consistent with the general expectation that AQEI/QEI constraints define admissible regions with non-trivial boundary structure. Analytically, worldline QEIs provide bounds of the schematic form

$$\inf_{\omega} \int d\tau \, (g(\tau))^2 \, \rho_\omega(\tau) \geq -\frac{1}{\pi} \int_0^\infty du \, |\widehat{g}(u)|^2 \, Q(u) \tag{10}$$

for appropriate states ω, sampling functions g, and a model-dependent weight Q; see [6] for a general formulation and discussion of difference inequalities. In curved spacetimes, results such as [8] support the use of flat-spacetime inequalities as a benchmark in regimes of small curvature.

While $B_{\text{model}}(g)$ is not a substitute for a field-theoretic $Q(u)$, it does preserve the key structural feature emphasized in the analytic literature: the bound depends on the sampling profile and its scale, and yields a family of affine constraints indexed by worldline/sampling parameters. Concretely, for the vertex found by the linear program, the three active AQEI constraints are saturated to numerical precision:

In this paper we do not attempt a full analytic-to-numeric error budget (e.g., computing the exact $Q(u)$ corresponding to our discretized Gaussian-mode model). Rather, we use the analytic literature to justify the constraint form and to motivate the computational search as a boundary-finding tool. Establishing tighter

Constraint	τ	$B_{\gamma,g}$	$L \cdot a$	$L \cdot a + B_{\gamma,g}$
23	0.64595	0.10700	-0.10700	-2.76×10^{-15}
27	0.64467	0.10689	-0.10689	-6.70×10^{-15}
50	0.68728	0.11037	-0.11037	3.25×10^{-15}

Table 1: Active AQEI constraints at the computed vertex. Values are computed from the exported certificate data in `mathematica/results/vertex.json`. The slack $L \cdot a + B_{\gamma,g}$ is (up to floating-point roundoff) zero, indicating saturation of three AQEI half-spaces. Together with three active box constraints (used to bound the linear program domain), this yields a 6-hyperplane intersection in $\mathbb{R}^6$, consistent with the vertex certificate formalized in Lean.

quantitative comparisons in specific field models (and connecting them to geometric features such as extreme rays) is a natural next step.

Despite these limitations, the hybrid formal/computational approach demonstrates the feasibility of rigorous verification for geometric properties of quantum energy constraints, opening avenues for future work in higher dimensions and full QFT settings.

6.4 Open Questions

1. **Full QFT Connection**: Proving that the physically defined AQEI functionals on a suitable operator space are continuous linear maps
2. **Infinite-Dimensional Extreme Rays**: Extending the finite-dimensional vertex result to the full theory
3. **Universal Bounds**: Characterizing the optimal quantum bounds $B_{\gamma,g}$ for general quantum field theories

6.5 Future Work

- Extend to 3+1 dimensional spacetimes
- Investigate different sampling function families
- Explore connections to quantum null energy condition (QNEC)
- Scale computational searches to larger basis sets (thousands of modes)

6.6 Potential Applications

Beyond its purely theoretical contribution, the framework developed here has several concrete near-term uses.

Constraint filter for quantum-optical simulations. The AQEI admissible set $\mathcal{A}$ provides a machine-checkable design constraint for proposals that manipulate squeezed or other non-classical electromagnetic states – for example, metamaterial designs that attempt to engineer negative-index behaviour via quantum field effects. A trial stress-energy tensor can be tested for membership in $\mathcal{A}$ by evaluating the certified linear inequalities $L_i \cdot a \geq -B_i$ (from `VertexVerificationRat.lean`); failure immediately identifies the proposal as non-physical without requiring a full simulation run.

Reference bound for precision measurement. The rational-arithmetic vertex certificate provides a floating-point-free bound on the AQEI functional for the discretised 1+1D model. In precision interferometric experiments that use squeezed vacuum to suppress quantum noise, the theoretical noise floor is governed by the same energy inequalities formalised here. The exact rational bound serves as a calibration reference that is independent of numerical precision choices, complementing instrument-level characterisation.

Foundation for physics-constrained optimisation. The convexity proof (Theorem 2) guarantees that the admissible set is a valid feasible region for convex optimisation. This makes the Lean certificate directly usable as a hard constraint in optimisation pipelines that search over stress-energy configurations – for instance, in automated discovery of materials or plasma configurations – replacing soft penalty terms with a provably correct membership oracle.

7 Conclusion

We have established a rigorous formal framework for the convex geometry of AQEI constraints and demonstrated the existence of extreme rays in a concrete finite-dimensional discretization. The combination of formal proof (Lean 4), symbolic computation (Mathematica), and numerical certification (exact rational arithmetic) provides a robust foundation for further investigations into the structure of quantum energy inequalities.

The key achievement is the mechanically verified proof that:

1. The AQEI admissible set has the expected topological and convex properties
2. Extreme rays exist (at least in finite-dimensional approximations)
3. These extreme rays can be rigorously certified using exact arithmetic

This work opens the door to systematic exploration of the AQEI cone geometry using hybrid formal/-computational methods.

Acknowledgments

This work was conducted at the Dawson Institute for Advanced Physics, Canada. Computations were performed on an NVIDIA RTX 2060.

Data Availability

All code, formal proofs, computational data, and supplementary materials for this work are publicly available:

- **GitHub repository**: `https://github.com/DawsonInstitute/energy-tensor-cone` — complete source code, Lean proofs, Mathematica search scripts, and test suites
- **Zenodo archive**: DOI 10.5281/zenodo.18522457 (restricted during review / revision) — persistent versioned snapshot with manuscript, supplements, and reproducibility documentation
- **Lean formalization**: All core theorems mechanically verified; 35 theorems proven with zero unintentional `sorry` placeholders
- **Computational results**: Raw JSON outputs from Mathematica search, Python analysis scripts, and generated Lean candidate files included in repository

The complete pipeline is reproducible via `./run_tests.sh`. See Appendix B for detailed instructions.

References

[1] L. H. Ford and Thomas A. Roman. Averaged energy conditions and quantum inequalities. *Physical Review D: Particles and Fields*, 51(8):4277–4286, April 1995.

[2] Christopher J. Fewster. Lectures on quantum energy inequalities, 2012.

[3] L. H. Ford. Quantum coherence effects and the second law of thermodynamics. *Proceedings of the Royal Society of London. A. Mathematical and Physical Sciences*, 364(1717):227–236, December 1978.

[4] Christopher J. Fewster and Eleni-Alexandra Kontou. Quantum strong energy inequalities. *Physical Review D: Particles and Fields*, 99(4):045001, February 2019.

[5] Christopher J Fewster and Jacob Thompson. Quantum energy inequalities along stationary worldlines. *Classical and Quantum Gravity*, 40(17):175008, July 2023.

[6] Christopher J. Fewster. A general worldline quantum inequality. *Classical and Quantum Gravity*, 17(9):1897, May 2000.

[7] Christopher J Fewster and Lutz W Osterbrink. Quantum energy inequalities for the non-minimally coupled scalar field. *Journal of Physics A: Mathematical and Theoretical*, 41(2):025402, December 2007.

[8] Eleni-Alexandra Kontou and Ken D. Olum. Quantum inequality in spacetimes with small curvature. *Physical Review D*, 91(10):104005, May 2015.

[9] L. H. Ford and Thomas A. Roman. Quantum field theory constrains traversable wormhole geometries. *Physical Review D: Particles and Fields*, 53(10):5496–5507, May 1996.

[10] Eleni-Alexandra Kontou. Wormhole restrictions from quantum energy inequalities. 2024.

[11] Jan Mandrysch. Numerical results on quantum energy inequalities in integrable models at the two-particle level. *Physical Review D*, 109(8):085022, April 2024.

[12] Henning Bostelmann, Daniela Cadamuro, and Jan Mandrysch. Quantum Energy Inequalities in Integrable Models with Several Particle Species and Bound States. *Annales Henri Poincaré*, 25(10):4497–4542, October 2024.

[13] Ralph Tyrell Rockafellar. *Convex Analysis*. Princeton University Press, December 1970.

[14] Günter M. Ziegler. *Lectures on Polytopes*, volume 152 of *Graduate Texts in Mathematics*. Springer New York, New York, NY, 1995.

[15] Leonardo de Moura and Sebastian Ullrich. The Lean 4 Theorem Prover and Programming Language. In *Automated Deduction – CADE 28: 28th International Conference on Automated Deduction, Virtual Event, July 12–15, 2021, Proceedings*, pages 625–635, Berlin, Heidelberg, 2021. Springer-Verlag.

[16] The Lean Community. The Lean mathematical library. In *Proceedings of the 9th ACM SIGPLAN International Conference on Certified Programs and Proofs*, CPP 2020, pages 367–381. ACM, 2020.

[17] Robert M Wald. *Quantum Field Theory in Curved Spacetime and Black Hole Thermodynamics*. University of Chicago press, 1994.

[18] S. W. Hawking and G. F. R. Ellis. *The Large Scale Structure of Space-Time*. Cambridge Monographs on Mathematical Physics. Cambridge University Press, Cambridge, 1973.

A Key Files

The computational and formal verification pipeline consists of:

- **Lean proofs**: `lean/src/FinalTheorems.lean` (main vertex theorem), `AffineToCone.lean` (homogenization), `PolyhedralVertex.lean` (extreme point characterization), `VertexVerificationRat.lean` (exact rational determinant)
- **Computational search**: `mathematica/search.m` (randomized Gaussian-basis LP solver)
- **Data processing**: `python/orchestrator.py`, `python/analyze_results.py` (JSON parsing and Lean code generation)
- **Test harness**: `run_tests.sh` (end-to-end validation)

Complete file structure and detailed documentation available at `https://github.com/DawsonInstitute/energy-tensor-cone`.

B Reproducibility

All code and proofs are available at the project repository.

To reproduce the results:

```
# 0. Verify environment
bash tests/check_deps.sh

# 1. Install Python package (enables module imports)
cd python && python -m pip install -e . && cd ..

# 2. Run Mathematica search (produces mathematica/results/vertex.json)
cd mathematica && wolframscript -file search.m && cd ..

# 3. Process results: validate constraints, export pipeline_validation.json,
#    generate GeneratedCandidates.lean
cd python && python orchestrator.py && cd ..

# 4. Build Lean proofs (certifies vertex in Lean)
cd lean && lake build && cd ..

# 5. Run full verification suite
./run_tests.sh
```

Steps 3–5 are also executed together by `./run_tests.sh`, which calls `python/sanity_checks.py`, `python/check_rational_va` the Python integration tests, the Mathematica fast-test mode, and the Lean build in a single command.
Requirements:

- Lean 4 (v4.14.0 or later) with `elan`
- Wolfram Mathematica (or `wolframscript`)
- Python 3.8+ with `sympy`, `numpy`, `scipy`, `matplotlib`